

The effects of upwelling over low SNR communications in shallow water

Fabio B. Louza and Sergio M. Jesus

Laboratory of Robotic Systems in Engineering and Science (LARSyS)

University of Algarve

8005-139 Faro, Portugal

fblouza@ualg.pt, sjesus@ualg.pt

Abstract—Coastal upwelling is a dynamical oceanographic process that severely modifies ocean temperature stratification, and, therefore, impacts acoustic propagation. The increasing ocean noise levels due to man-made activities not only contribute to hamper the acoustic modem performance but also affect marine life. The impacts of oceanographic processes over communications are not well understood. This paper presents a study on the effects of coastal upwelling over low SNR communications in shallow water. The focus is on the role of ocean temperature stratification induced by the upwelling regime off the Cabo Frio Island (Brazil) over broadband low power coherent modulated signals. Based on data from the BioCom'19 experiment, numerical simulations using the Monterey-Miami Parabolic Equation model (MMPE) were used to compare the acoustic propagation for typical sound speed profiles, indicating a complex channel to establish communications. Furthermore, low SNR communication performance was correlated to the temperature profiles during the experiment. The resulting bit error rates show that temporal averaging of recorded low power signals was able to cope with this challenging environment.

Index Terms—Coastal upwelling, Underwater communications

I. INTRODUCTION

Coastal upwelling is a dynamical oceanographic process that severely modifies ocean temperature stratification, inducing the movement of cold water towards the sea surface [1]. Previous work reported in the literature have studied and described the functioning of wind-driven coastal upwelling mechanism in several specific locations across the ocean, due to its ecological consequences, carrying nutrient-rich subsurface water into the euphotic zone, increasing substantially the biological productivity, and therefore, fishing activities [1], [2]. However, the influence of oceanographic parameters over acoustic propagation and communication performance is not well understood. Therefore, a study based on ocean modeling to understand the role of upwelling in creating shadow coastal zones, reducing the probability of detection of an acoustic source, is presented in [3]. Another work using noncoherent acoustic communication signals showed that the thermocline variability may explain the differences in the modem performance, in terms of bit-error rate (BER) [4]. Furthermore, the rising concerns about the impacts of man-made noise on marine life have motivated studies about low power signals for communications [5], [6].

In this study, the main objective is to understand the effects of the coastal upwelling over low SNR communications in shallow water. To support the analysis, a small subset of data from the shallow water BioCom'19 experiment [7] was used. The range-dependent bathymetry includes a depression at mid-distance between the source and receivers through which the cold water sips into the region.

During the experiment, several sound speed profiles (SSP) were acquired along the propagation track. The temperature profiles were also continuously monitored along the water column at the receiver location. Furthermore, broadband low power coherent bitstreams were continuously transmitted and recorded on a pyramidal array of four hydrophones. Simulations using the Monterey-Miami Parabolic Equation model (MMPE) [8] were used to compare the acoustic propagation for upwelling regime SSP. The resulting transmission loss (TL) plots and predicted CIR indicated a complex channel to establish communications, depending on the ocean temperature stratification. Moreover, an analysis was performed to correlate the SNR to the temperature profiles during the experiment. The resulting bit error rates show that temporal averaging of recorded signals was able to cope with this challenging environment.

II. COASTAL UPWELLING OFF THE CABO FRIO ISLAND

The wind-driven coastal upwelling off the Cabo Frio island is a complex oceanographic mechanism triggered by the action of the predominant NE/E wind blowing regime, inducing offshore movement of surface water and, therefore, the ascending motion of cold and deep water towards the ocean surface [2], [3]. In the Southern hemisphere, as a consequence of the Ekman transport, the integrated flow of the near-surface ocean points 90° angle to the left of the wind. Furthermore, there is an inflection of the Brazilian coast from NE/SW to E/W direction at the vicinities of the Cabo Frio region, extending hundreds of km in a straight coastline, and a continental shelf break topography that favors the phenomena. Therefore, the coast-parallel component of the wind stress induces the offshore transport of water in the surface Ekman layers, rising the South Atlantic Central Water (SACW) towards the sea surface until a dynamical equilibrium is reached. The upwelling is more intense in summer/spring due to the shallowness of the thermocline and the prevalence of NE/E

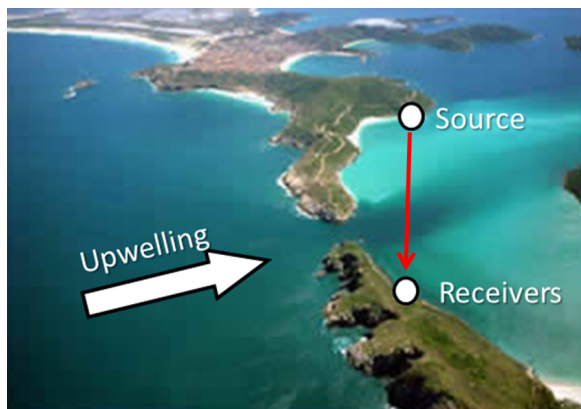


Fig. 1. BioCom'19 experiment shallow water site, off the Cabo Frio Island (Brazil). The propagation track, in red, crosses the valley (darker area in the picture) through which cold water sips into the bay.

winds in these seasons [2]. The upwelling phenomena have several implications, changing the marine biota and impacting the ocean temperature stratification. Despite covering just 1% of the ocean, the regions of occurrence are the most productive, contributing around 20% of fishing activities [2]. Furthermore, the sound speed in the ocean is a function of pressure (depth), temperature and salinity, $c = f(p, t, s)$ [9]. Therefore, the mixing of the water masses of different compositions strongly affects the sound speed profiles, influencing the propagation of acoustic signals used for communications.

III. THE BIOCOM'19 EXPERIMENT

The BioCom'19 experiment took place in a semi-enclosed shallow water bay, off the Cabo Frio Island (Brazil) from Jan14-18, 2019 (Fig. 1). The source was placed at mid-water in a 4 m deep water column, and the pyramidal array of four hydrophones was located 1.6 km away from the source. The hydrophones were mounted on a pyramidal frame of 1m-long edge, posed at the bottom in an 8 m water column. The strong currents flowing in and out of the bay through the Boqueirão strait created a bathymetric depression (valley) at mid-distance between the source and receivers, shown as the darker area in Fig. 1. To monitor the upwelling, several SSP were acquired by a CTD at three locations (source, valley, and receiver), reaching depths varying from 4-20m. Furthermore, a time-series of temperature profiles were continuously recorded along the water column at the receiver location (Fig. 2).

Low power superimposed training bitstreams composed of a long m-sequence laid over to the data were transmitted once every 5 minutes [6]. Used as pilot signals, m-sequences are orthogonal codes that provide an impulse-like autocorrelation suitable for signal synchronization and channel estimation. The communication signals with a central frequency of 7.5 kHz and bandwidth of 3 kHz were emitted from an omnidirectional acoustic source 55 times per minute to explore temporal diversity and to perform error correction through coherent averaging. In shallow water, the acoustic energy interacts several times with ocean boundaries, sea surface, and bottom,

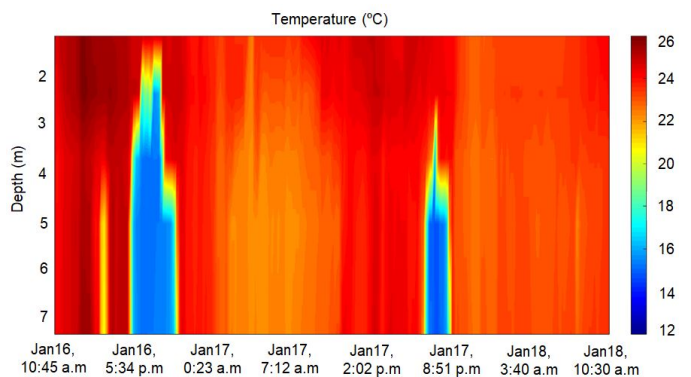


Fig. 2. Time-series of temperature profiles along the water column at the receiver location, recorded from Jan16, 10:45 a.m. to Jan18, 10:30 a.m. Short-term drastic temperature changes of more than 10 degrees Celsius in a few hours indicate the upwelling occurrences.

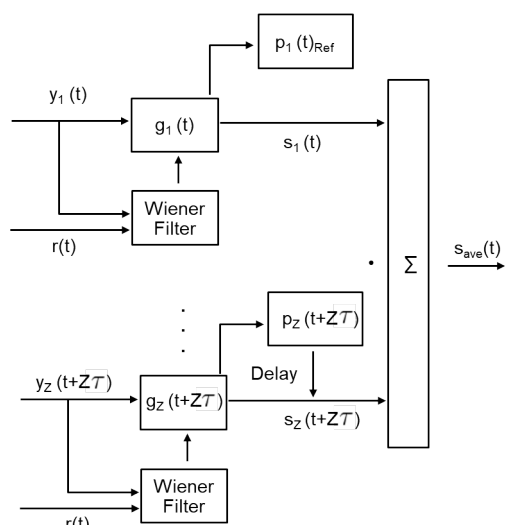


Fig. 3. Diagram of Wiener filtering of superimposed training bitstreams, matched filtering for synchronization and coherent averaging in time.

inducing multiple replicas at the receiver. This multipath severely degrades the communication system performance. Thus, each received sequence $y_z(t + z\tau)$ was equalized with an inverse Wiener filter to mitigate multipath, where z is the sequence number and τ is the period of the transmitted bitstream. Then, the filtered $g_z(t + z\tau)$ were matched filtered with the m-sequence probe $r(t)$. Based on the strongest peak of the cross-correlation results $p_z(t + z\tau)$, the bitstreams $s_z(t + z\tau)$ were synchronized (time-aligned). To achieve a high processing gain at the receiver the bitstreams were coherently averaged. The error-corrected signal $S_{ave}(t)$ was processed and the data retrieved [6] (Fig. 3).

IV. THE ACOUSTIC PROPAGATION IN AN UPWELLING SCENARIO

In order to understand the acoustic propagation in this complex environment, the communication channel was modeled using typical geological parameters and approximate

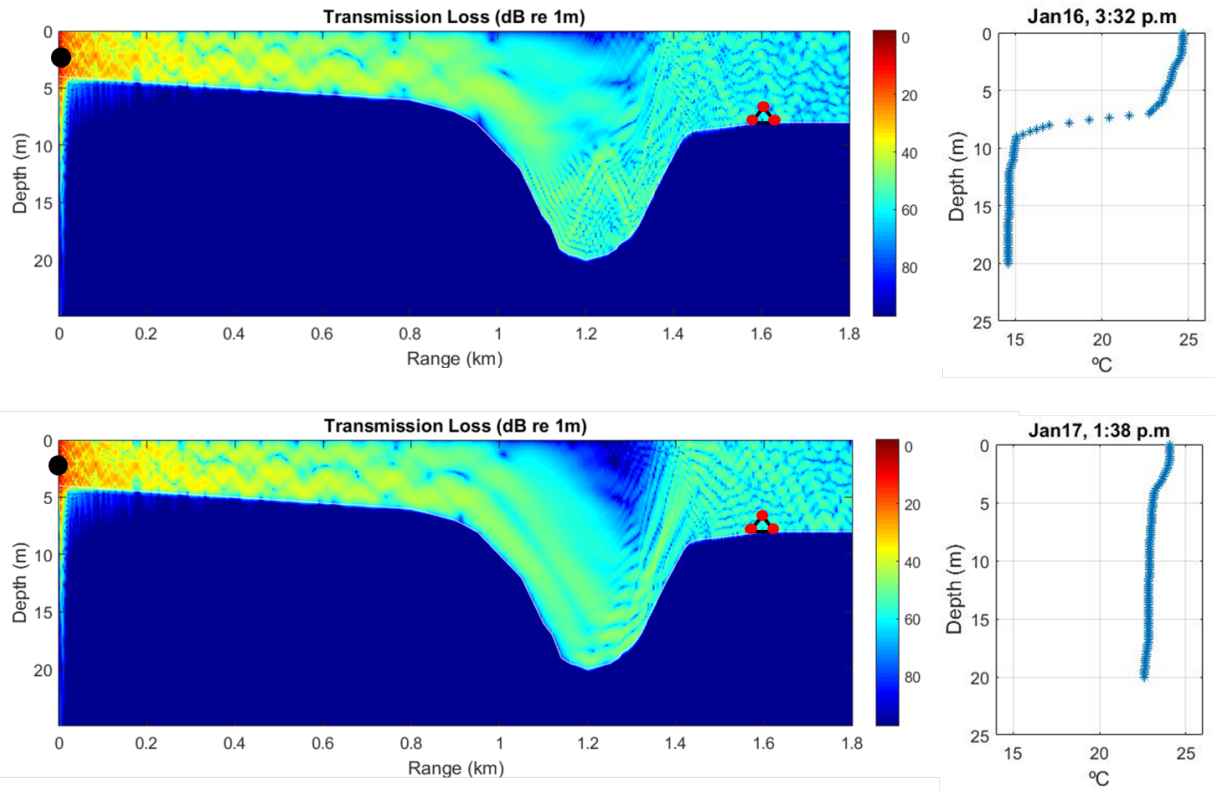


Fig. 4. Numerical estimations of transmission loss (TL) using the MMPE acoustic model ($f_c = 7.5kHz$, $BW = 3kHz$). The source (black dot) is placed mid-water in a 4 m deep water column. The pyramidal array (red dots) is located 1.6 km far from the source, posed at the bottom in an 8 m water column. Calculations were performed for an upwelling SSP recorded on Jan16, 3:32 p.m (top plot), and a slightly downward refracting SSP from Jan17, 1:38 p.m (bottom plot).

bathymetry for the experimental site. Based on the Cabo Frio region substratum composition [10], the bottom was assumed as medium sand with a compressional speed of 1671 m/s. Two representatives SSP, upwelling (Fig. 4 (top plot, right)) and slightly downward refractive (Fig. 4 (bottom plot, right)), collected from CTD at the depression on Jan16, 3:32 p.m., and Jan17, 1:38 p.m. were inserted in the MMPE model to simulate the propagation for the same center frequency and bandwidth of the real signals. For both SSP, the transmission loss (TL) plots show multiple interactions of the acoustic energy with the bottom and sea surface, between the source and the valley (Fig. 4, left). However, along this deeper region, for the upwelling condition, the propagation is much different. As one can observe in Fig. 4 (top plot, right)), at the depth of 9m, there is an abrupt reduction of temperature of approximately 10°C in just 3m, creating two layers of distinct propagation. Therefore, TL plot shows that most of the energy refracts towards the bottom and becomes trapped in this depression, reducing significantly the energy available at the hydrophones (Fig. 4 (top plot, left)). Conversely, for the slightly downward refracting SSP, the energy propagates following the bottom geometry, and therefore more energy reaches the hydrophones (Fig. 4 (bottom plot, left)).

The results of the TL predicted by the MMPE model are in agreement with data from the experiment. Fig. 5 and 6 show

both the CIR estimated from data recorded by hydrophone #1 (three plots on the left) and the noiseless CIR predicted by the MMPE acoustic model (plot on the right), for the upwelling and slightly downward refracting SSP, respectively. For the upwelling SSP condition (Jan17, 7 p.m), Fig. 5 (left) shows the 55 estimated CIR. The noisy CIR exhibit low amplitudes and a time-varying fading. Several bitstreams cannot be even detected, as one can observe between seconds 10 to 20. On the other hand, for a slightly downward refracting SSP (Jan17, 2 p.m), the estimated CIR show higher amplitudes. In an almost isothermal condition, all bitstreams were detected, pointing to a more stable propagation channel with hydrophones receiving more energy (Fig. 6 (left)). To observe the multipath structure, the two plots in the middle of Fig. 5 and 6 focus on two specific CIR, indicated by the red dots. For the upwelling SSP, the low SNR CIR #33 and #50 present a long delay spread of approximately 10 ms, including a strong arrival much before the most significant peak that complicates the synchronization and equalization processes. However, for the slightly downward refracting SSP, the CIR #12 and #42 present a higher SNR, showing more energetic arrivals and a shorter multipath compared to the upwelling CIR. In Fig. 5 and 6 (right), the CIR predicted by MMPE show the fading and multipath structure in agreement with the estimated CIR. The communication system uses several consecutive m-sequences

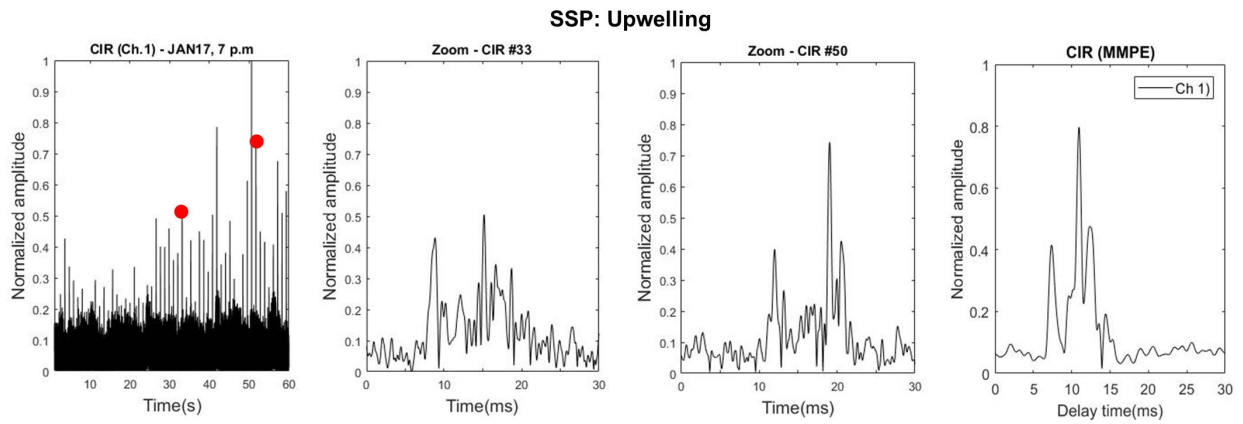


Fig. 5. The first three plots on the left show the CIR estimated from the 55 bitstreams recorded by hydrophone #1, and the multipath structure for the sequences #33 and #50 (red dots). On the right, a CIR shows the multipath arrivals predicted by the MMPE model, for a depth of 7m, approximately the same as hydrophone #1. (SSP: upwelling).

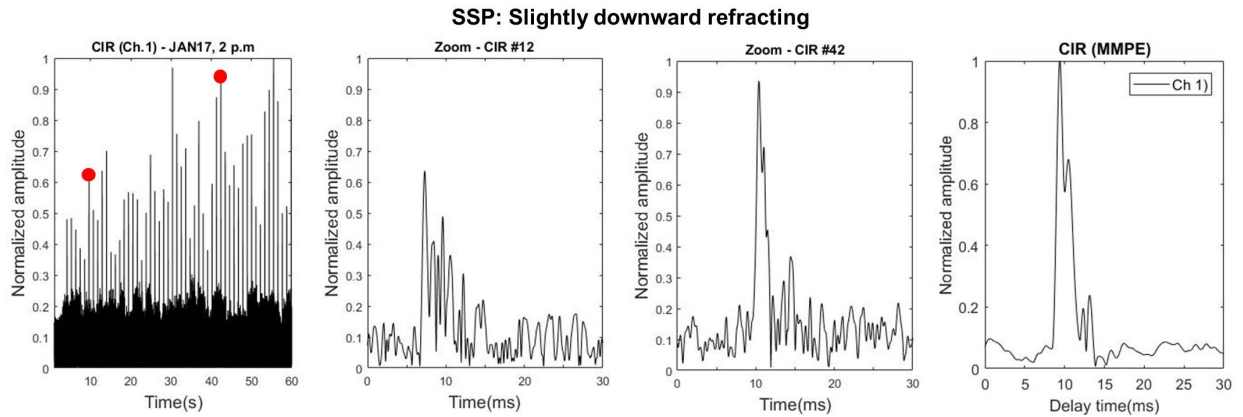


Fig. 6. The first three plots on the left show the CIR estimated from the 55 bitstreams recorded by hydrophone #1, and the multipath structure for the sequences #12 and #42 (red dots). On the right, a CIR shows the multipath arrivals predicted by the MMPE model, for a depth of 7m, approximately the same as hydrophone #1. (SSP: slightly downward refracting).

to estimate the channel. Performing a comparison, one can observe a high degree of similarity between the CIR from MMPE and the CIR #50 and #42 from real data. This is an interesting result and may validate the accuracy of the numerical simulation, based on real data.

V. TEMPERATURE EVOLUTION VS. COMMUNICATION PERFORMANCE

Coherent communications are generally affected by Doppler effects. However, in this experiment, as the source and receiver were maintained steady in the water, signal processing was performed using zero Doppler probe replicas. The in-band SNR (dB) for channel #1 was estimated according to $SNR = 10 \log_{10} [(S - N)/N]$, where S is the mean of the signal plus noise power of 20 sequences, N is the mean of the noise power of a sequence of the same length of S , estimated from a period after transmissions.

For the time window from Jan17, 1 p.m. to Jan18, 7 a.m., the SNR or temperature vs. time plot (Fig. 7 (top plot)) shows a direct correlation between the upwelling and the

signal power measured by the hydrophone #1 and the sensor temperature close to the top of the array. Observing the SNR and temperature evolution in time, the SNR starts to decline several hours before the cold water reaches the array location. This may be an indicator of the upwelling occurrence. As cold water sips into the bay, the temperature stratification along the propagation track changes so that more energy refracts to the bottom and becomes trapped into the depression. Conversely, as the channel evolves to an almost isothermal condition (slightly downward refracting SSP), the SNR increases as more energy reaches the sensors.

In addition to the ocean temperature stratification, the high noise levels in the region, related to both man-made and biological factors, and the severe multipath structure that changes for each received signal also contributed to hampering the demodulation of the received low power signals. In agreement with the SNR evolution, Fig. 7 (bottom plot) shows the BER estimated from hydrophone #1. To evaluate the system robustness and to perform error correction in this challenging environment, the BER were estimated using 20 bitstreams (22

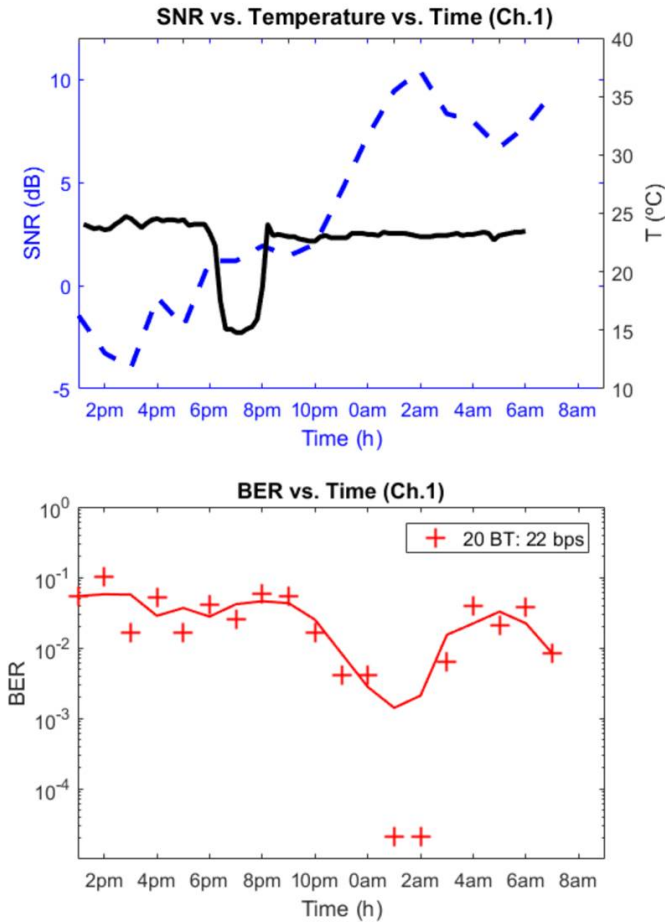


Fig. 7. Top plot: – SNR vs. Temperature vs. Time measured at the array location from Jan17, 1 p.m. to Jan18, 7 a.m. The dashed line (blue) indicates SNR estimated by the hydrophone #1 using 20 bitstreams. Superimposed to the SNR, the temperature profile (black) estimated by the sensor close to the top of the array. Bottom plot: BER vs. Time for an effective bit rate of 22 bps, equivalent to averaging for 22 seconds (20 bitstreams). The red line represents a smooth fitting curve of data.

bps). A large range of SNR (-5.2 to 9.1 dB) was observed. During the upwelling, as propagation conditions changed, the system achieved $BER > 10^{-2}$. But, as the channel returned to a more stable condition, SNR increased and the communication system retrieved $BER < 10^{-2}$, including error-free messages, for consecutive hours. The higher the SNR, the lower the BER.

VI. CONCLUSIONS

In this paper, we studied the effects of the upwelling oceanographic phenomena over low SNR communications in shallow water. Based on a small subset of data from the BioCom'19 experiment, a time series of temperature profiles at the receiver location was plotted to indicate the upwelling events. The acoustic propagation for the upwelling and slightly downward refracting SSP were simulated using the Monterey-Miami parabolic equation model. The TL plot indicated a severe multipath in both situations, but a reduction of available

energy at the receiver for the upwelling SSP, as the sound became trapped inside the depression through which the cold water sips into the bay. These model results are in agreement with the estimated CIR from hydrophone #1 for both SSP. The authors analyzed the SNR vs. temperature vs. time and the BER plots for the hydrophone at the top of the array. A reduction of the SNR indicates the occurrence of the upwelling where water masses of different temperatures mix, affecting the propagation. The achieved BER were in agreement with the evolution of the SNR for selected bit rate. The higher the SNR, the lower the BER.

Future work will perform an analysis of the influence of oceanographic parameters over communications using each channel, independently, and all four hydrophones combined to observe the performance and suitability of this small array for this environment. Improving knowledge about the effects of upwelling over low SNR communication signals using an easy-to-deploy pyramidal array may help to develop communication systems suitable for sensors operating in these harsh environments, saving power and reducing acoustic pollution. Furthermore, the communication system may be used, indirectly, to monitor the upwelling phenomena using low power acoustic signals, instead of conventional temperature sensors. Moreover, taking advantage of spatial averaging may lead to lower BER, improving the robustness of the communication system.

ACKNOWLEDGMENT

This paper was funded by the Postgraduate Study Abroad Program of the Brazilian Navy, Grant No. Port.227/MB/2019, and by the National Council for Scientific and Technological Development (CNPq)/Science without Borders Program (Contract No. 401407/2014-4). This work was also supported by Fundação para a Ciência e a Tecnologia (FCT) through LARSyS - FCT Project UIDB/50009/2020.

REFERENCES

- [1] J. Kämpf and P. Chapman, "The functioning of coastal upwelling systems," in *Upwelling Systems of the World (Springer International Publishing)*, 2016, pp. 31–66.
- [2] S. Coelho-Souza, M. S. López, J. D. Guimarães, R. Coutinho, and R. N. Candella, "Biophysical interactions in the Cabo Frio upwelling system, southeastern Brazil," *Brazilian Journal of Oceanography*, vol. 60, pp. 353–365, 2012.
- [3] L. Calado, O. Rodriguez, G. Codato, and F. Xavier, "Upwelling regime off the Cabo Frio region in Brazil and impact on acoustic propagation," *J. Acoust. Soc. Am.*, vol. 143, no. 3, p. 174, 2018.
- [4] M. Siderius, M. B. Porter, P. Hursky, V. McDonald, and the KauaiEx Group, "Effects of ocean thermocline variability on noncoherent underwater acoustic communications," *J. Acoust. Soc. Am.*, vol. 121, no. 4, pp. 1895–1908, Apr. 2007.
- [5] R. Diamant and L. Lampe, "Low Probability of Detection for Underwater Acoustic Communication: A Review," *IEEE Access*, vol. 6, pp. 19 099–19 112, 2018.
- [6] F. B. Louza and H. A. DeFerrari, "Superimposed training low probability of detection underwater communications," *J. Acoust. Soc. Am.*, vol. 148, no. 3, pp. EL273–EL278, Sep. 2020.
- [7] F. B. Louza, J. Osowsky, F. C. Xavier, E. E. Vale, L. P. Maia, R. P. Vio, M. V. S. Simões, V. Barroso, and S. M. Jesus, "Communications and biological monitoring experiment in an upwelling environment at cabo frio island bay," in *OCEANS 2019 - Marseille*, 2019, pp. 1–7.

- [8] K. B. Smith and F. D. Tappert, "UMPE: The University of Miami Parabolic Equation Model, Version 1.1 - MPL Technical Memorandum 432," 1994.
- [9] C.-T. A. Chen and F. Millero, "Speed of sound in seawater at high pressures," *Journal of The Acoustical Society of America - J ACOUST SOC AMER*, vol. 62, pp. 1129–1135, 11 1977.
- [10] I. S. Simões, F. Xavier, L. Barreira, L. Artusi, H. Macedo, Y. Alvarez, R. Romano, and J. Hermand, "Medições geoacústicas em sedimentos marinhos da plataforma continental proxima a Arraial do Cabo—RJ," in *Jornadas de Engenharia Hidrografica*, Lisboa, Portugal, 2012.